

Envelope Gene-Mediated Neurovirulence in Feline Immunodeficiency Virus Infection: Induction of Matrix Metalloproteinases and Neuronal Injury

J. B. Johnston, C. Silva, and C. Power*

Department of Clinical Neurosciences, University of Calgary, Calgary, Alberta, Canada

Received 26 April 2001/Accepted 5 December 2001

The release of neurotoxins by activated brain macrophages or microglia is one mechanism proposed to contribute to the development of neurological disease following infection by lentiviruses, including feline immunodeficiency virus (FIV). Since molecular diversity in the lentiviral envelope gene influences the expression of host molecules implicated in neuronal injury, the role of the envelope sequence in FIV neuropathogenesis was investigated by using the neurovirulent FIV strain VICSF, the nonneurovirulent strain Petaluma, and a chimera (FIVCh) containing the VICSF envelope gene in a Petaluma background. All three viruses replicated in primary feline macrophages with equal efficiency, but conditioned medium from VICSF- or FIVCh-infected cells was significantly more neurotoxic than medium from Petaluma-infected cultures ($P < 0.001$) and could be attenuated in a dose-dependent manner by treatment with either the matrix metalloproteinase (MMP) inhibitor prinomastat (PMT) or function-blocking antibodies to MMP-2. Although FIV sequences were detectable by PCR in brain tissue from neonatal cats infected with each of the viral strains, immunohistochemistry revealed increased astrogliosis and macrophage activation in the brains of VICSF- and FIVCh-infected cats relative to the other groups, together with elevated markers of neuronal stress that included morphological changes and increased *c-fos* immunoreactivity. Similarly, MMP-2, but not MMP-9, mRNA and protein expression was increased in brain tissues of VICSF- and FIVCh-infected cats relative to Petaluma-infected animals ($P < 0.01$). Infection with VICSF or FIVCh was also associated with greater CD4⁺ cell depletion ($P < 0.001$) and neurodevelopmental delays ($P < 0.005$), than in Petaluma-infected animals; these deficits improved following PMT therapy. These findings indicated that diversity in the envelope gene sequence influenced the neurovirulence exhibited by FIV both in vitro and in vivo, possibly through a mechanism involving the differential induction of MMP-2.

Feline immunodeficiency virus (FIV) is a lentivirus that causes immunological and neurological impairment in domestic cats similar to that seen in human immunodeficiency virus (HIV)-infected patients (2). FIV is neurotropic, entering the central nervous system (CNS) during the early stages of infection and primarily targeting microglia and brain macrophages (15). In 20 to 40% of naturally infected felines, invasion of the CNS by FIV is characterized by neurological abnormalities, such as convulsions, ataxia, reduced motor activity, disorientation, and altered sensory evoked potentials, as well as behavioral abnormalities, such as psychomotor slowing, aggressiveness, disrupted sleep and arousal patterns, and stereotypic motor behavior (38, 45). Although overt clinical signs of neurological disease are not exhibited by all FIV-infected cats, neuronal injury and loss, inflammation, altered blood-brain barrier (BBB) integrity, white matter pallor, and multifocal gliosis are apparent in many animals upon necropsy (38). In general, the neuropathological complications of FIV infection are less prominent than those observed with primate lentiviruses, but the similarities in these features suggest that these viruses share a common neuropathogenesis (55).

Genomic variability that tends to cluster within distinct regions of the envelope gene has been demonstrated for several

lentiviruses during the course of persistent infection and has been shown to have important ramifications for viral pathogenesis (1, 8, 10, 11, 27). For example, small amino acid changes in the surface unit (SU) or transmembrane (TM) glycoprotein of FIV determine cell tropism (30, 36, 52–54), receptor profiles (59), and cytopathogenicity (30, 36). Similar regions within the envelope gene have also been shown to influence the development of neurological disease in various retroviral systems, conferring a neurovirulent phenotype on otherwise nonneurovirulent viral strains (27, 31, 42, 49). Although the basis for these phenotypic differences is unclear, several studies have implicated the ability of these regions to influence cell tropism (4, 9, 48, 52) and the release of toxic molecules by infected cells (14, 26, 29, 43). However, as with HIV, the potential for differences in envelope sequences to modulate the pathogenesis of FIV in vivo, although proposed to occur (41), has been poorly characterized.

The mechanisms by which FIV envelope proteins may contribute to the development of neurological disease are not known, but both direct and indirect pathways have been proposed. For example, FIV envelope proteins have been shown to be neurotoxic when applied directly to neuronal cultures (6, 20). In addition, FIV infection alters intracellular signaling pathways and host cell regulation of several putative neurotoxins, including proteolytic enzymes, glutamate, chemokines, and proinflammatory cytokines (24, 40, 61, 62). The expression of many of these molecules has also been shown to vary with the

* Corresponding author. Mailing address: Department of Clinical Neurosciences, HMRB 150, 3330 Hospital Dr. NW, University of Calgary, Calgary, Alberta, Canada T2N 4N1. Phone: (403) 220-5572. Fax: (403) 283-8731. E-mail: power@ucalgary.ca.

FIV strain and with specific sequences in the viral envelope (24, 41), further supporting a role for envelope diversity in the pathogenesis of FIV. Ultimately, however, neuronal death is thought to involve viral proteins or host-derived factors that influence glutamate uptake, neurotransmitter release, or calcium exchange (4, 6, 20, 61). Recently, matrix metalloproteinases (MMPs), a family of proteolytic enzymes posited to contribute to CNS disease by promoting the degradation of basement membranes, a breakdown in BBB integrity, and neuronal death (60), have been implicated in the neuropathogenesis of lentiviruses (3, 12, 24, 25). Moreover, expression of these enzymes was shown to depend on specific sequences within the envelope genes of both HIV and FIV and to mediate the neuropathogenic properties of lentivirus infections (24, 25). However, no direct link between envelope-dependent MMP expression and the neurotoxicity associated with some FIV strains has been shown.

Using a neonatal feline model, our laboratory previously demonstrated that the neurovirulence associated with FIV is viral strain dependent (41). Animals infected with V1CSF, a novel cerebrospinal fluid (CSF)-derived FIV isolate, exhibited greater neurodevelopmental delays and neuropathological changes than neonates infected with the blood-derived Petaluma strain of FIV. Moreover, compared to Petaluma infection, infection of primary feline macrophages by V1CSF resulted in enhanced production of putative neurotoxins, such as MMPs, through a mechanism that was influenced by the sequence of the FIV envelope gene (24). In the present study, an envelope chimera, FIVCh, was used to demonstrate that the differences in neurovirulence exhibited by V1CSF and Petaluma resulted from diversity within the FIV envelope gene. Furthermore, like that of HIV, the neurotoxicity exhibited by FIV was found to be attenuated by inhibitors of MMP activity, indicating a common mechanism in the pathogenesis of neurovirulent lentiviruses.

MATERIALS AND METHODS

Cell culture. Peripheral blood mononuclear cells (PBMC) used for infection studies and preparation of viral stocks were isolated from blood obtained from specific-pathogen-free adult felines by density gradient centrifugation, as described previously (23). PBMC were initially stimulated for 3 days with concanavalin A (5 μ g/ml; Sigma, Oakville, Ontario, Canada) and then maintained in RPMI 1640 medium with 15% fetal calf serum (FCS) and interleukin-2 (100 IU/ml; Sigma). Primary monocyte-derived macrophages (MDM) were isolated from unstimulated PBMC by adherence on polystyrene flasks for 24 h, differentiated for 7 days, and cultured in RPMI 1640 medium containing 20% FCS. NG-108 mouse neuroblastoma cells were obtained from the American Type Culture Collection (Manassas, Va.) and cultured in minimal essential medium containing 10% FCS. All cell cultures were supplemented with antibiotics.

Viruses and infection. The FIV strains used in this study included the primary isolate V1CSF, which was derived from the CSF of a cat with encephalopathy (41) and underwent fewer than 10 passages in feline PBMC prior to the present experiments to minimize the effects of culture adaptation. Virus was also obtained from infectious molecular clones of FIV by transfection into CrFK cells and selection in feline PBMC as described previously (24). These viruses included a hybrid of two molecular clones of the blood-derived Petaluma strain of FIV (37), pFIV-34TF10 and pFIV-14 (National Institutes of Health AIDS Research and Reference Reagent Program); the hybrid was constructed by replacing sequences encoding the ORFA gene (nucleotides [nt] 5328 to 6393) of pFIV-34TF10 with equivalent sequences from pFIV-14. As a result, the hybrid lacked both the 8 kb of extraneous cellular DNA incorporated into pFIV-14 and the stop codon present in the ORFA gene of pFIV-34TF10. Similarly, an envelope chimera of V1CSF and Petaluma, FIVCh (24), was generated by exchanging the envelope gene of the Petaluma hybrid (nt 6393 to 8906) with that of V1CSF.

Culture supernatants from FIV-infected feline PBMC, which served as sources of infectious virus for these experiments, were cleared of cellular debris by centrifugation and titered by limiting dilution as described previously (23). For infection with FIV, primary MDM were inoculated with 200 μ l of viral stock ($10^{2.5}$ to $10^{4.5}$ 50% tissue culture infectious doses [TCID₅₀/ml], incubated for 2 h at 37°C, washed twice, and cultured in serum-free medium until supernatants (conditioned media [CM]) and cells were harvested. Infection was assessed by measuring reverse transcriptase (RT) activity in CM as described previously (24).

Neurotoxicity assay. NG108 neuroblastoma cells (5×10^4 /well) were seeded in 96-well plates in serum-free medium, differentiated by incubation with 1 mM dibutyryl cyclic AMP (Sigma) for 24 h, and incubated for 24 h with CM harvested at days 1 and 3 postinfection (p.i.) from mock- and FIV-infected feline MDM. These time points were selected based on previous experiments demonstrating that the *in vitro* neurotoxicity induced by FIV reaches its peak before day 4 p.i. (41). Following exposure to CM, cultures were stained with trypan blue dye (Sigma) for 15 min at room temperature, and the number of cells which failed to exclude the dye were counted in 4 wells (3 to 6 fields per well; 0.1 mm²/field) by an observer unaware of the treatment identity. Neuronal death was determined by the number of stained cells expressed as a percentage (mean \pm standard error of the mean [SEM]) of the total number of cells counted (equalized to control values). A consistent level of background cell death (3 to 5%) was observed between experiments. To assess the role of MMPs in FIV-induced neurotoxicity, CM from FIV- and mock-infected feline MDM were pretreated for 1 h at room temperature either with the MMP inhibitor prinomastat (PMT; AG3340) (25, 47) or with a function-blocking antibody to MMP-2. Antibodies or PMT diluted in fresh culture media served as controls for nonspecific cytotoxicity. The antibody to MMP-2 (Oncogene Research Products, Cambridge, Mass.) was used at concentrations of 0 to 8 μ g/ml based on the manufacturer's suggestions and dose-response experiments. The MMP-2 antibody was shown previously to recognize both the latent (72-kDa) and active (66-kDa) forms of the enzyme and not to cross-react with other known gelatinases, such as MMP-9 (25, 28, 51). PMT (Agouron Pharmaceuticals, Inc., San Diego, Calif.) was used at concentrations of 0 to 25 μ M.

Animals and virus inoculation. Adult specific-pathogen-free pregnant cats (queens) were obtained from Unique Ventures (Winnipeg, Manitoba, Canada) and housed according to University of Calgary Animal Resource Center guidelines. All queens were found to be negative for feline retroviruses by PCR analysis and serological testing. At day 1 postdelivery, neonatal kittens were inoculated intraperitoneally or intracranially (right frontal lobe) with 0.2 ml of infectious ($10^{4.5}$ TCID₅₀/ml) or heat-inactivated virus by using a 30-gauge needle and syringe. Only one viral strain was used for each litter in order to avoid cross-contamination, and at least two litters were infected per viral strain. To assess the role of MMPs in FIV-induced neurological disease, four FIVCh-infected animals received daily intraperitoneal injections of PMT (50 mg/kg), starting at 6 weeks, until the completion of the experiment (12 weeks). Kittens were weaned at 6 weeks and monitored until the age of 12 weeks; during this period, changes in body weight were assessed weekly. PBMC were isolated from blood collected at 8 and 12 weeks p.i.; FIV infection was determined by PCR analysis, and levels of CD4⁺ and CD8⁺ cells were investigated by flow cytometry. After 12 weeks, animals were euthanized, and brain and spleen tissues were harvested. Three animals infected with FIVCh were perfused with normal saline prior to extraction of brain tissue. Samples from each animal were either fixed in 4% buffered (pH 7.4) paraformaldehyde or frozen immediately by immersion in liquid nitrogen for immunocytochemical and PCR analyses, respectively.

PCR and RT-PCR analyses. Genomic DNA was isolated from tissue or cultured cells by using the DNeasy reagent (Gibco, Burlington, Ontario, Canada) according to the manufacturer's protocols. Total cellular RNA was isolated by using the TRIzol reagent (Gibco) and was treated with DNase (1 U/ μ g) for 1 h at 37°C, and the absence of contaminating cellular DNA was confirmed by PCR using the conditions and primers described below. cDNA was prepared from 100 ng of treated RNA by using a First Strand cDNA Synthesis kit (Boehringer Mannheim) with a poly(dT) primer alone or in combination with a primer targeting a specific gene. For semiquantitative PCR, approximately 300 to 400 ng of template DNA or cDNA was amplified by 1 cycle of 95°C for 5 min (denaturation); 30 cycles of 95°C for 1 min, 50 to 65°C for 1 min, and 72°C for 2 min (amplification); and 1 cycle of 72°C for 10 min (extension). Nested PCR was performed by using 2 μ l of product amplified in the first PCR with the same reagents and reaction conditions. To minimize the possibility of contamination, PCRs were prepared in one room, templates were added in a second, and the actual PCR amplification was conducted in a third area. As a contamination control for each reaction, 2 μ l of water was added to the reaction mixture instead of the template. Loading of equal amounts of template from each sample was ensured by amplification of the host gene, glyceraldehyde-3-phosphate dehydro-

genase (GAPDH). To optimize the number of cycles and amount of template necessary for amplification within the linear range of detection of the PCR protocol, standard curves were generated for all primer pairs using serial dilutions of template from control samples (24). The sequences of all primers and probes used to detect the FIV *pol* gene (23) and MMP-2, MMP-9, and tumor necrosis factor alpha (TNF- α) (25) have been reported previously.

Southern blot and densitometric analyses. PCR products were separated by agarose gel electrophoresis, transferred to nylon membranes via capillary action, and probed with an [α - 32 P]dCTP-labeled oligonucleotide probe specific for each virus or host gene, as described previously (24, 25). DNA and cDNA levels were quantitated by densitometric analysis of a minimum of three Southern blots from separate experiments. Briefly, blots were scanned in grey scale at high resolution (>600 dpi; Hewlett-Packard ScanJet 6300C) and optical density was measured with Scion Image image processing and analysis software. Levels of each host or viral gene were normalized to the corresponding GAPDH level for statistical analysis and compared to standards with known concentrations. Standards were included on all membranes to calibrate for relative transfer and exposure efficiency and to allow comparison between blots.

Immunocytochemistry. Paraformaldehyde-fixed brain tissue, collected at necropsy from mock- and FIV-infected animals, was cryoprotected by immersion in 30% sucrose for 3 days. Serial, free-floating (30- μ m-thick) sections (frontal cortex and white matter) were prepared by using a sliding microtome and were stored at 4°C in phosphate-buffered saline (PBS) containing 0.04% sodium azide. In preparation for use, sections were washed with PBS and then incubated for 30 min at room temperature in 3% hydrogen peroxide. Sections were washed again and incubated for 45 min at room temperature in blocking solution containing 10% normal goat serum (NGS; Sigma) and 0.4% Triton X-100 in PBS. Following the blocking step, tissue sections were incubated for 24 to 48 h with a primary antibody diluted in PBS containing 5% NGS and 0.4% Triton X-100, washed, and incubated for 2 h with a secondary antibody diluted in PBS containing 1.5% NGS. Primary antibodies used for these studies included glial fibrillary acidic protein (GFAP; 1:5,000; Dako Diagnostics, Mississauga, Ontario, Canada), *c-fos* (1:10,000; Oncogene Research Products, Boston, Mass.), microtubule-associated protein 2 (MAP-2; 1:5,000; Sigma), and CD18 (1:100; provided by Peter Moore, University of California, Davis). Monoclonal and polyclonal antibodies were detected by using horseradish peroxidase-conjugated goat anti-mouse (Jackson ImmunoResearch Lab) or anti-rabbit (Sigma) secondary antibodies, respectively, and were visualized by incubation with diaminobenzidine and hydrogen peroxide.

Tissue zymography. pro-MMP protein levels in brain tissue from mock- and FIV-infected neonates were determined by gelatin zymography as described previously (24). Briefly, protein extracts (75 μ g) were separated by electrophoresis on a sodium dodecyl sulfate-8% polyacrylamide gel that was copolymerized with 1 mg of gelatin (Difco, Detroit, Ill.)/ml. Gels were agitated for 1 h in renaturing buffer containing 2.5% Triton X-100 to restore enzymatic activity and then incubated for 24 h at 37°C in buffer lacking detergent. Gelatinase activity on gels stained with Coomassie blue was detectable as unstained bands representing areas of gelatin digestion. Stained gels were dried, and pro-MMP abundance was determined by densitometry. Standards were generated previously by zymography and densitometric analysis to ensure that MMP detection was within the linear range.

Flow cytometry. Whole blood was collected in K₃-EDTA tubes and incubated for 5 min at room temperature with four parts of ammonium chloride lysing solution (17 mM NH₄Cl, 100 mM KHCO₃, 0.1 mM EDTA) to lyse erythrocytes. PBMC were pelleted by centrifugation, resuspended in PBS containing 0.1% sodium azide (10⁶ cells), and incubated for 20 min at room temperature with anti-CD4 or CD8 monoclonal antibodies (3 μ g/ml; kindly provided by Peter Moore, University of California, Davis). Cells were again washed, incubated for 20 min with fluorescein isothiocyanate-conjugated goat anti-mouse immunoglobulin G (0.25 μ g/ μ l; Becton Dickinson, San Jose, Calif.), and resuspended in 0.5 ml of 1% formalin in PBS for analysis. By use of a FacScan flow cytometer (Becton Dickinson) with the argon laser excitation set at 488 nm, data were collected from approximately 15,000 events for each experimental condition, and results were expressed as a single-parameter log fluorescence histogram. Cells incubated in the absence of antibodies or with 1 μ g of fluorescein isothiocyanate-labeled, isotype-matched murine immunoglobulin G1 (Becton Dickinson)/ml served as controls.

Neurodevelopmental studies. To assess the development of neurological disease, FIV- and mock-infected kittens were examined weekly by animal care staff unaware of their infection status, and the ages at which animals were able to successfully complete specific neurodevelopmental tasks (running, jumping, air righting, plank walking, and blink reflex) were determined. Neurodevelopmental impairment was expressed as a score on a mean disability scale (MDS) (21) on

which values between 0.5 and 1.0 indicate normal development. These scores were calculated based on results obtained between weeks 6 and 12 p.i. and represented the mean number of standard deviations by which values for animals in each group differed from previous control values (41).

Statistical analyses. Statistical analyses were performed using Graphpad Prism, version 3.0, for Windows (Graphpad Software, San Diego, Calif.). For comparisons of three or more unmatched groups, one-way analysis of variance (ANOVA) was performed, followed by a Tukey-Kramer multiple-comparison posttest to determine differences between specific groups. For data derived from two groups, Student's *t* test was used. *P* values of <0.05 were considered significant for all tests.

RESULTS

MDM tropism of parent and chimeric FIV strains. Because the release of neurotoxins by infected and/or activated macrophages has been posited to contribute to the neuronal injury induced by FIV (62), primary feline MDM were infected with V1CSF, FIVCh, or Petaluma and viral replication was determined by measuring RT activity in CM. Peak activity was detected at day 9 p.i. for all three viruses, with no significant differences observed among FIV strains at any of the time-points (Fig. 1a). Thus, like primary feline PBMC (24), both parent and chimeric viruses replicated equally well in feline MDM.

CM from FIV-infected feline MDM are neurotoxic. Previously, V1CSF was shown to cause higher levels of cell death in *in vitro* neurotoxicity assays than the primary isolate of Petaluma (41). To compare the relative abilities of the parent and chimeric viruses used in this study to induce production of potential neurotoxins by macrophages, neurotoxicity was assessed by using CM harvested at days 1 and 3 p.i. from feline MDM infected with V1CSF, Petaluma, or FIVCh. These time points were chosen based on earlier *in vitro* studies that investigated cell death in neuronal cultures treated for varying incubation periods with CM harvested at different days p.i. (41). Relative to that in untreated cultures and cultures treated with CM from mock-infected MDM, neuronal death was increased following incubation with CM from MDM infected with any of the FIV strains (Fig. 1b). Although neurotoxicity did not differ between cultures incubated with media harvested on day 1 versus day 3 p.i., differences were detected between viruses. CM harvested at day 3 p.i. from V1CSF-infected MDM and CM harvested at the same time point from FIVCh-infected MDM caused equivalent levels of cell death (25.3 \pm 3.1 and 22.5 \pm 3.1%), which were significantly higher (*P* < 0.001) than that caused by media from Petaluma-infected cells (11.4 \pm 2.3%). Similar results were observed for samples from day 1 p.i., suggesting that the ability to induce the release of neurotoxins differed between the FIV strains despite similar tropisms for feline macrophages.

Inhibition of MMPs blocks FIV-induced neurotoxicity *in vitro*. Previously, it was demonstrated that FIV infection of feline MDM induced expression of both MMP-2 and -9 that was greater in cultures infected with V1CSF or FIVCh than in Petaluma-infected cells (24). To investigate a potential role for MMPs in the neurotoxicity exhibited by FIV *in vitro*, CM from FIV- and mock-infected feline MDM were treated with PMT, an MMP inhibitor previously shown to inhibit the neurotoxicity associated with HIV (25), and then applied to neuronal cultures. Pretreatment with PMT significantly reduced the neurotoxicity associated with CM from MDM infected with

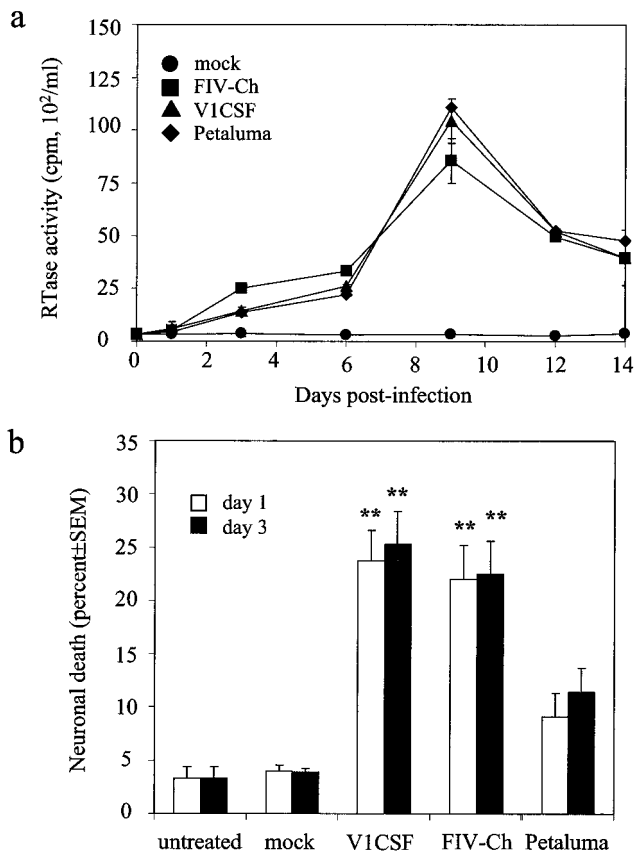


FIG. 1. In vitro macrophage tropism and neurotoxicity of FIV strains. Primary feline MDM were infected with Petaluma, V1CSF, or FIVCh at 10^{4.5} TCID₅₀/ml, and culture supernatants were harvested at successive days p.i. Mock-infected cultures served as controls. (a) Viral replication was assessed by RT assay at days 3, 6, 9, 12, and 14 p.i. and was expressed as the mean ± SEM (counts per minute per milliliter) of triplicate samples from three independent wells. Significant differences relative to control cultures were determined by ANOVA and a Tukey-Kramer post-hoc test (*P* < 0.001 at all time-points for each virus). All three viruses replicated equally well in feline MDM. (b) Differentiated NG108 neuroblastoma cells were incubated for 24 h with supernatants harvested at day 1 or 3 p.i. from mock- or FIV-infected feline MDM. Cells incubated with fresh medium (untreated) served as controls for background neurotoxicity. Cell death in each well was determined by trypan blue exclusion and equalized for the total number of cells. Each result represents trypan blue-positive cells as a percentage of total cells detected (mean ± SEM for three wells [four fields/well]). Significant differences relative to neurons treated with supernatants from Petaluma-infected MDM were determined by ANOVA and the Tukey-Kramer post-hoc test (**, *P* < 0.001; *, *P* < 0.01). Greater neurotoxicity was observed with supernatants from V1CSF- or FIVCh-infected MDM than with those from Petaluma-infected cells on both days.

V1CSF (49%) or FIVCh (39%) (Fig. 2a). Furthermore, as illustrated for V1CSF in Fig. 2b, this effect was dose dependent. In contrast, PMT did not have a significant effect on the neurotoxicity associated with Petaluma.

PMT is a selective MMP inhibitor that exhibits picomolar affinities for gelatinases; thus, it inhibits the activities of both MMP-2 and MMP-9 (47). Although FIV infection of MDM increases MMP-9 expression, previous reports have demonstrated that, unlike MMP-2, this enzyme does not participate in lentivirus-mediated neurotoxicity (25, 56). To determine if

MMP-2 plays a role in FIV-mediated neuronal death, CM from FIV- or mock-infected feline MDM were pretreated with function-blocking antibodies to MMP-2 prior to application to neuronal cultures. Anti-MMP-2 antibodies reduced the level of neuronal death associated with V1CSF or FIVCh by almost the same amount as PMT (39 and 32%, respectively) (Fig. 2a). As with PMT, this effect was dose dependent (Fig. 2b) and was not observed when CM from Petaluma-infected cells were treated. Of note, no differences in cell death were observed between neuronal cultures incubated with PMT or MMP-2 antibodies diluted in fresh medium and cells incubated with medium alone. These results suggested that the differences in

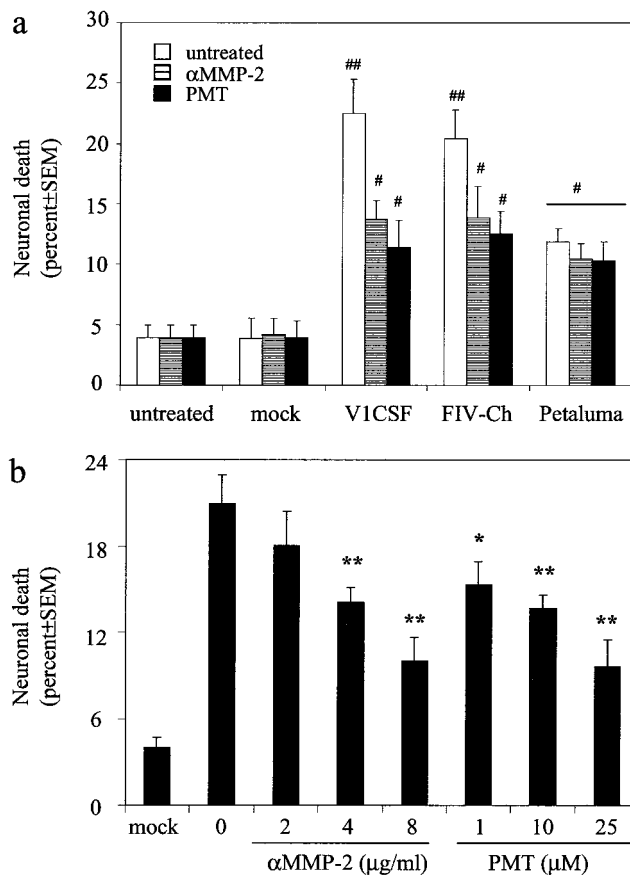


FIG. 2. MMP inhibition attenuates FIV-induced neurotoxicity. Differentiated NG108 neuroblastoma cells were incubated for 24 h with supernatants harvested at day 3 p.i. from mock- or FIV-infected feline MDM in the presence or absence of anti-MMP-2 antibodies (αMMP-2, 0 to 8 μg/ml) or PMT (0 to 25 μM). Cells incubated with fresh medium (untreated) served as controls for background neurotoxicity. Cell death in each well was determined by trypan blue exclusion and equalized for the total number of cells. Each result represents trypan blue-positive cells as a percentage of total cells detected (mean ± SEM for three wells [four fields/well]). (a) The neurotoxicity associated with V1CSF or FIVCh, but not Petaluma, was inhibited by both anti-MMP-2 antibodies (8 μg/ml) and PMT (25 μM). Significant differences relative to cultures treated with supernatants from mock-infected cultures were determined by ANOVA and the Tukey-Kramer post-hoc test (##, *P* < 0.001; #, *P* < 0.01). (b) Both anti-MMP-2 antibodies and PMT inhibited V1CSF-associated neurotoxicity in a dose-dependent manner. Significant differences relative to untreated cultures (0) were determined by ANOVA and the Tukey-Kramer post-hoc test (**, *P* < 0.001; *, *P* < 0.01).

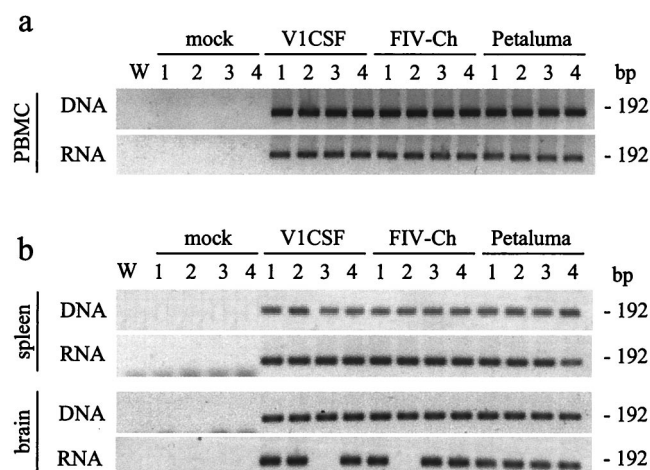


FIG. 3. Detection of FIV sequences in PBMC and tissues from FIV-infected neonates. PBMC (a) and necropsied brain (frontal lobe) and spleen tissues (b) were obtained at 12 weeks p.i. from mock ($n = 8$), Petaluma ($n = 6$), V1CSF ($n = 6$), and FIVCh ($n = 7$)-infected neonates. Genomic DNA and total cellular RNA, from which cDNA was made, were isolated and the presence of the FIV *pol* gene was confirmed by nested PCR and Southern blot detection. Representative blots for three independent reactions are shown for four animals in each group. A water blank (W) served as a contamination control. FIVCh-infected animals 2 and 3 were infected by intraperitoneal injection. All other animals received virus intracranially. Viral DNA was detected in all tissues from each FIV-infected group but not in mock-infected controls. However, FIV RNA was detectable only sporadically in brain tissues from neonates infected with V1CSF or FIVCh.

neurotoxicity exhibited by the FIV strains resulted from the preferential abilities of V1CSF and FIVCh to induce MMP-2 expression due to the envelope genes they encoded.

Infection of neonates with parental and chimeric FIV strains. To assess the profile of FIV infection in vivo, neonatal kittens were infected with parental or chimeric viruses by intracranial or intraperitoneal injection and evidence of FIV infection, including detection of virus and systemic immunosuppression, was measured over 12 weeks. Nested PCR analysis of genomic DNA and total cellular RNA from PBMC harvested at weeks 8 (data not shown) and 12 (Fig. 3a) p.i. detected the presence of virus-specific sequences at both time points in all FIV-infected animals. Similarly, FIV sequences were detectable at week 12 p.i. in matched brain and spleen samples collected at necropsy from infected animals (Fig. 3b). In contrast, FIV was not detected in cells or tissue samples from any of the mock-infected controls. Although FIV was detected in genomic DNA from brain tissues obtained from all infected animals, FIV sequences were present in brains at the RNA level only sporadically (in six of six Petaluma-infected animals, four of six V1CSF-infected animals, and five of seven FIVCh-infected animals).

FIV infection of neonatal brain tissue is associated with gliosis and neuronal stress. The morphological changes associated with the neurological impairment observed in FIV-infected neonates were investigated by immunocytochemical analysis of serial sections of necropsied frontal lobe brain tissue from mock-infected animals and cats infected with parental or chimeric virus. GFAP immunoreactivity was increased in the brains of FIV-infected cats, which demonstrated astrocyte

hypertrophy and an increased number of detectable processes compared to those in control brains (Fig. 4a through d). Similarly, evidence of increased macrophage activation in infected animals compared to controls was provided by the ability to detect a greater number of cells that were immunopositive for CD18, which labels monocytes and lymphocytes (Fig. 4e through h). However, the extents of astrogliosis and macrophage activation were markedly increased in animals infected with V1CSF or FIVCh over those in Petaluma-infected cats. Although neuronal loss was not obvious in any FIV-infected group, immunostaining with antibodies to MAP-2 revealed dysmorphic neurons, characterized by shorter and less-abundant processes, in animals infected with V1CSF and FIVCh (Fig. 5a through d). Additional evidence of neuronal stress, such as increased immunoreactivity to the transcription factor *c-fos*, was also detected in V1CSF- and FIVCh-infected brain tissue compared to Petaluma- and mock-infected brains (Fig. 5e through h). Of note, *c-fos* staining was observed primarily in the nuclei of neurons, with limited cytoplasmic staining. In addition, only isolated *c-fos*-positive cells were detected in Petaluma- and mock-infected brains, while clusters of positive neurons were evident in V1CSF- and FIVCh-infected animals (Fig. 5).

MMP expression is elevated in brain tissues from FIV-infected neonates. Previously, increased MMP expression was reported in brain tissues from both FIV-infected adult cats and HIV-infected patients who were diagnosed with lentivirus-induced neurological disease (24). To determine if the neurodevelopmental impairment detected in neonates was associated with a similar increase in MMP levels, the expression of MMPs implicated in the development of neurological disease was assessed in brain tissues from the FIV- and mock-infected neonates described above. RT-PCR (Fig. 6a) and tissue zymography (Fig. 6b) revealed that MMP-2 and -9 mRNA and proenzyme protein levels were increased in FIV-infected felines over levels in controls. Although pro-MMP-9 expression did not differ between infected animals (an increase of approximately 4-fold with all viruses), the increases in levels of pro-MMP-2 were greater in felines infected with V1CSF (3.7-fold \pm 0.5-fold) or FIVCh (3.6-fold \pm 0.4-fold) than in Petaluma-infected animals (1.8-fold \pm 0.5-fold) ($P < 0.005$) (Fig. 6c). Similarly, expression of the proinflammatory cytokine TNF- α was also elevated in FIV-infected brain tissues over that in controls, with higher mRNA levels in animals infected with V1CSF ($P < 0.01$) or FIVCh ($P < 0.05$) than in the Petaluma-infected group.

Systemic changes in FIV-infected neonates. The systemic features of FIV infection were assessed by measuring changes in body weight and peripheral blood cell populations over the 12-week period. Weekly determinations of body weights indicated that progressive weight gains occurred in both mock- and FIV-infected animals (Fig. 7a). However, the mean weight for each of the FIV-infected groups was significantly lower than that for control animals, while V1CSF-infected animals also exhibited decreased weight gains compared to both Petaluma ($P < 0.05$)- and FIVCh ($P < 0.05$)-infected cats. In contrast, no significant differences were observed between Petaluma- and FIVCh-infected animals.

Analysis by flow cytometry of PBMC isolated at week 8 p.i. from FIV- and mock-infected cats revealed no significant dif-

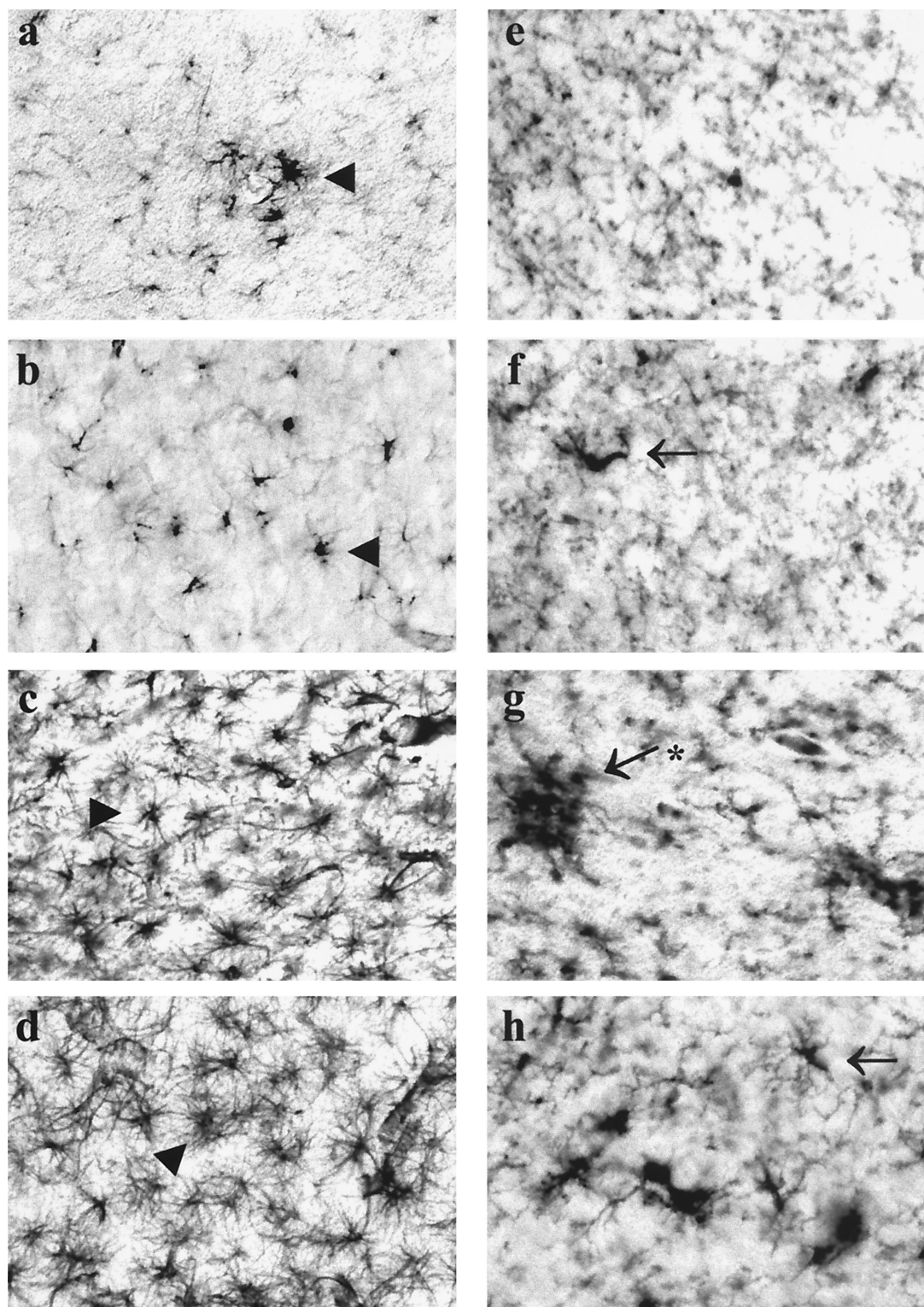


FIG. 4. Gliosis and macrophage activation in FIV-infected brain tissue. Serial sections of brain tissue (frontal lobe) collected at 12 weeks p.i. from mock (a and e)-, Petaluma (b and f)-, V1CSF (c and g)-, or FIVCh (d and h)-infected neonates were immunostained with antibodies to GFAP (a, b, c, and d) or CD18 (e, f, g, and h). Increased GFAP immunoreactivity, indicative of astrogliosis, was detected in V1CSF- and FIVCh-infected brains compared to mock- and Petaluma-infected brains. Similarly, CD18 immunostaining revealed that activated macrophages were more abundant in animals infected with V1CSF or FIVCh than in the other groups. Original magnification, $\times 200$. Arrowheads, hypertrophic astrocytes; arrows, activated macrophages or microglia; asterisk, microglial nodule.

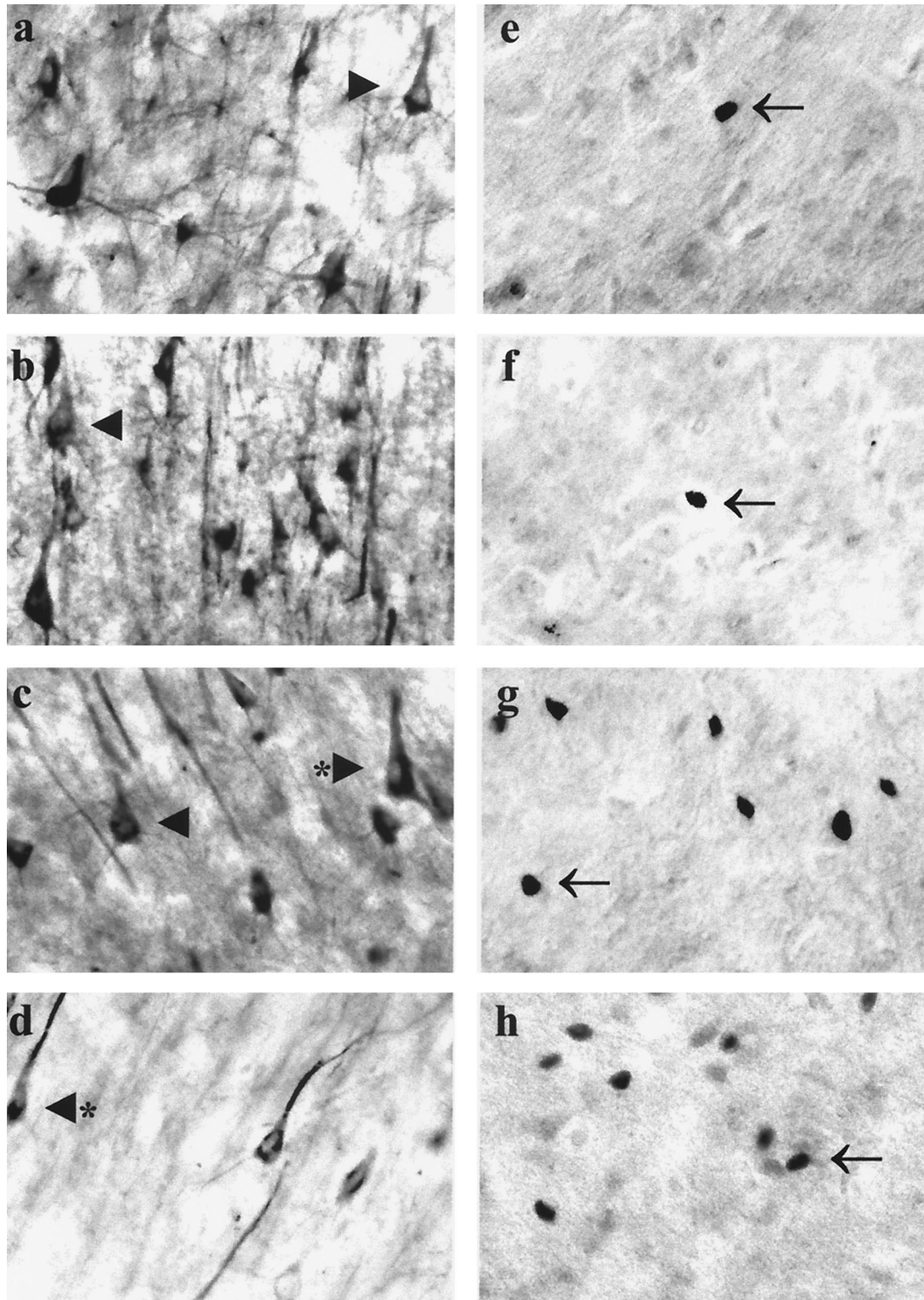


FIG. 5. Neuronal damage and stress in FIV-infected feline brain tissue. Serial sections of brain tissue (frontal lobe) collected at 12 weeks p.i. from mock (a and e)-, Petaluma (b and f)-, V1CSF (c and g)-, or FIVCh (d and h)-infected neonates were immunostained with antibodies to MAP-2 (a, b, c, and d) or *c-fos* (e, f, g, and h). Although minimal neuronal loss was observed in FIV-infected animals compared to mock-infected controls, dysmorphic neurons were more evident in V1CSF- and FIVCh-infected animals than in the other groups. Similarly, increased *c-fos* immunoreactivity, localized primarily to the nuclei of neurons, was detected in neonates infected with V1CSF or FIVCh, with isolated, positively stained neurons observed infrequently in mock- or Petaluma-infected brain tissue. Original magnification, $\times 400$. Arrowheads, healthy neurons; asterisks, dysmorphic neurons; arrows, *c-fos*-positive nuclei.

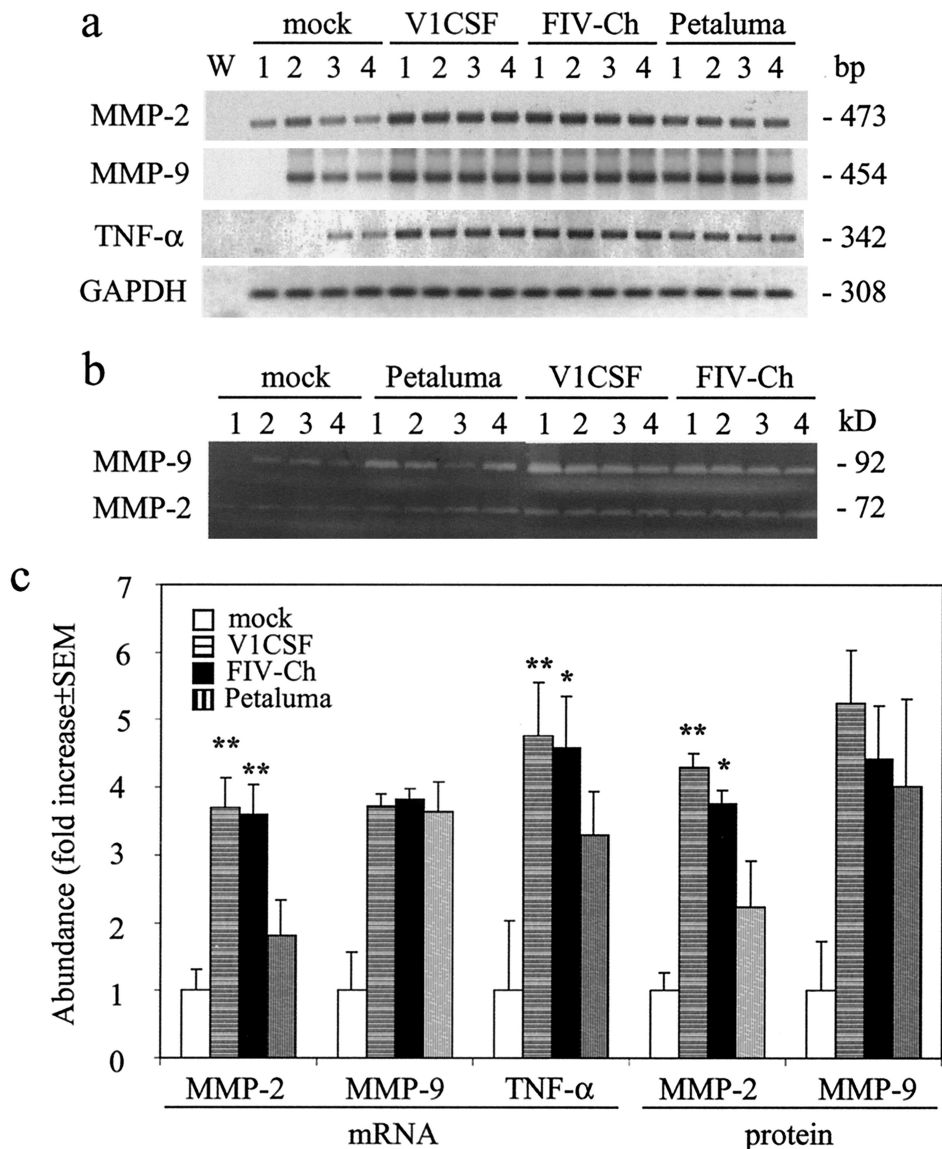


FIG. 6. MMP expression in FIV-infected brain tissue. Protein and RNA, from which cDNA was prepared, were extracted from brain tissues (frontal lobe) harvested at 12 weeks p.i. from mock-infected neonates and cats infected with Petaluma, V1CSF, or FIVCh. mRNA and protein expression was determined by semiquantitative RT-PCR and gelatin zymography, respectively, and results from four animals in each group are shown. (a) Representative blots indicating increased MMP-2 and TNF-α mRNA levels in neonates infected with V1CSF or FIVCh compared to levels in mock- and Petaluma-infected animals. Amplification of a water blank (W) and of RNA isolated from each sample preparation prior to making cDNA ensured the lack of contaminating DNA. (b) Representative zymograms indicating similarly elevated pro-MMP-2 and pro-MMP-9 protein levels. (c) Densitometric analysis of RNA and pro-MMP protein levels, expressed as the mean density ± SEM in arbitrary units following equalization for GAPDH RNA levels or total protein abundance in each sample. Significant differences relative to Petaluma-infected animals (**, $P < 0.01$; *, $P < 0.05$) were determined by ANOVA and the Tukey-Kramer post-hoc test.

ferences between groups in the percentage (15% [Fig. 7b]) or absolute number (approximately 800 cells/μl [data not shown]) of CD4⁺ cells. In contrast, CD4⁺ cell levels were significantly lower at week 12 p.i. ($P < 0.001$) in animals infected with V1CSF or FIVCh than in mock- and Petaluma-infected cats. These differences reflected an increase in the number of CD4⁺ cells in Petaluma-infected and control animals (13 and 80%, respectively), while levels in V1CSF- and FIVCh-infected animals decreased over the same period (50% for both groups). Comparison of CD8⁺ cells at the same time-points indicated that levels were increased significantly in all FIV-infected groups compared to controls at week 8 p.i. (Fig. 7c), with levels

in FIVCh-infected cats (22% ± 2%) exceeding those in animals infected with V1CSF (10% ± 2%) or Petaluma (16% ± 3%). By week 12 p.i., CD8⁺ cells, which had increased by 31 and 150% in Petaluma- and mock-infected animals, respectively, were elevated significantly in Petaluma-infected animals compared to the other groups. The percentage of CD8⁺ cells in cats infected with V1CSF or FIVCh remained stable in both groups between weeks 8 and 12 but remained higher than levels in controls. Taken together, these results indicated that the FIVCh chimera was infectious in vivo and had the capacity to cause systemic disease characterized by immunosuppression.

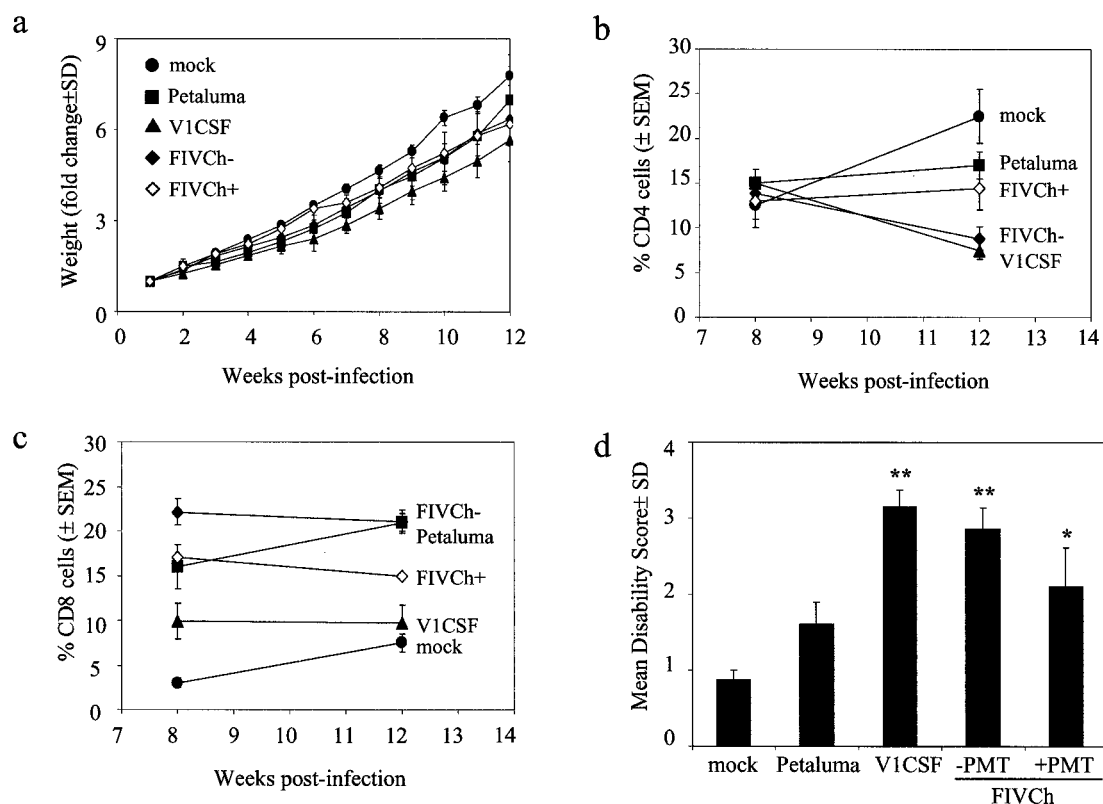


FIG. 7. Systemic and neurodevelopmental changes in FIV-infected neonates. (a) Mock- and FIV-infected neonates were assessed weekly, and weight changes were measured relative to the starting weight (week 1) for each animal. Data represent the mean \pm standard deviation for each group. Significant differences relative to mock-infected cats were determined by Student's *t* test. V1CSF-infected animals exhibited decreased weight gains compared to mock-infected cats ($P < 0.005$) and cats infected with the other FIV strains ($P < 0.05$). No differences were observed between Petaluma-infected animals and cats infected with chimeric virus but not treated with PMT (FIVCh-), but weight gains were reduced in both groups relative to controls ($P < 0.05$). Treatment of FIVCh-infected cats with PMT (FIVCh+) resulted in increased weight gains over those in untreated animals, but this effect was not observed after 6 weeks p.i. (b and c) PBMC were isolated from whole blood collected at weeks 8 and 12 p.i., and the numbers of CD4⁺ (b) and CD8⁺ (c) cells were determined by flow cytometry. Results are expressed as the mean percentage \pm SEM of labeled cells relative to the total number of PBMC. CD4 levels in V1CSF-infected cats and cats infected with FIVCh in the absence of PMT were significantly decreased ($P < 0.001$) at week 12 p.i. compared to levels in mock- and Petaluma-infected animals and PMT-treated cats infected with FIVCh. CD8 levels increased in mock- and Petaluma-infected animals and decreased in cats infected with the other viruses between weeks 8 and 12 but remained elevated in Petaluma- and FIVCh-infected animals relative to mock- and V1CSF-infected neonates at both time points ($P < 0.001$). Treatment with PMT reversed the loss of CD4⁺ cells detected in FIVCh-infected animals but did not affect CD8⁺ cell levels. (d) Developmental parameters (play interaction, walking, running, jumping, air righting, blink reflex, plank walking) were measured weekly for 12 weeks, and impairment was scored based on the mean age (in weeks) at which animals in each group were able to successfully complete a given task. Results represent the MDS \pm standard deviation for each group. Significant differences relative to mock-infected animals were determined by Student's *t* test (*, $P < 0.05$; **, $P < 0.005$). A significant degree of impairment was observed in animals infected with V1CSF or FIVCh, but not in Petaluma-infected cats. Treatment with PMT decreased the extent of impairment detected in FIVCh-infected neonates.

Neurodevelopmental impairment in FIV-infected neonates.

To assess in vivo neurovirulence, induction of neurological disease in neonatal cats infected with the parental and chimeric viruses was determined by using a neonatal feline model of neurodevelopmental impairment. Compared to mock-infected controls, which had an MDS score of 0.9 ± 0.1 , animals infected with any of the FIV strains exhibited evidence of developmental delays (Fig. 7d). Consistent with a previous study using the primary isolate of Petaluma (41), animals infected with V1CSF presented with a level of impairment (3.2 ± 0.2) that was significantly greater ($P < 0.005$) than that observed for Petaluma-infected cats (1.6 ± 0.3). As with CD4⁺ cell depletion, neonates infected with FIVCh exhibited a level of impairment (2.9 ± 0.3) similar to that of V1CSF-infected animals, exceeding that induced by Petaluma ($P < 0.005$) (Fig. 7d). Differences between FIV- and mock-infected neonates

manifested primarily as the delayed acquisition of the ability to complete jumping, blink reflex, and plank walk tasks. Furthermore, as with systemic changes, no differences were observed in the development of neurological disease when animals from different litters were infected with the same virus or when neonates were inoculated by intraperitoneal versus intracranial routes.

PMT therapy attenuates the systemic and neurodevelopmental changes associated with FIV infection. To determine if inhibition of MMPs influenced the course of FIV-induced illness in vivo, neonates infected with FIVCh ($n = 4$) were treated daily with PMT (75 mg/kg of body weight) and systemic and neurodevelopmental changes were assessed as previously. PMT-treated neonates exhibited weight gains comparable to those observed with mock-infected controls during the first 6 weeks p.i. (Fig. 7a), but no differences were observed between

treated and untreated animals at later time points. In contrast to the CD4 cell depletion detected in untreated animals, CD4⁺ cell levels in FIVCh-infected cats receiving PMT increased between weeks 8 and 12 p.i. (Fig. 7b), although CD8⁺ cell levels remained stable in both treated and untreated groups over the same period (Fig. 7c). Furthermore, neonates treated with PMT exhibited near-significant decreases in MDS scores compared to untreated FIVCh-infected cats (2.1 ± 0.5 versus 2.9 ± 0.3), supporting the *in vitro* results suggesting a role for MMPs in FIV-induced neurotoxicity.

DISCUSSION

The present study demonstrates that diversity within the envelope gene is an important determinant of the viral strain-specific nature of the neurovirulence exhibited by FIV. Infection of feline MDM by V1CSF and FIVCh, viruses expressing the envelope gene of V1CSF, was associated with increased production of putative neurotoxins, such as MMP-2, and higher levels of neurotoxicity, than infection by Petaluma. These same molecules were elevated preferentially in brain tissues from V1CSF- and FIVCh-infected neonates, concurrent with evidence of neuronal injury. Following infection of neonatal cats, both V1CSF and FIVCh induced more severe neurological impairment and CD4 cell depletion than the Petaluma strain of FIV, an effect that was attenuated by treatment with the MMP-2 inhibitor PMT. These results suggest that individual FIV strains differ in their capacities to induce neurological disease *in vivo* and *in vitro* due to variability in envelope sequence.

In addition to neurovirulence, systemic abnormalities in the form of decreased levels of peripheral CD4⁺ cells were also associated with the development of neurological disease in animals infected with FIVCh, which was similar to findings for V1CSF (41). Although FIVCh-infected animals exhibited weight gains that were comparable to those of Petaluma-infected cats, depletion of immune cells was not detected to the same extent in the latter group, suggesting that systemic immunosuppression following FIV infection was also influenced by the viral strain and envelope sequence. The importance of this finding is illustrated by an earlier report from our laboratory demonstrating that Petaluma-induced neurological impairment is enhanced in neonates immunosuppressed by cyclosporine A therapy (41). Therefore, the results of the present study further support the concept that the ability to cause immunosuppression may be a requisite feature of the neurovirulent phenotype associated with V1CSF and FIVCh.

It is unlikely that the differences observed between the FIV strains used in this study are solely a product of differences in viral replication, since all three viruses exhibited similar tropisms for feline MDM and PBMC *in vitro*. Furthermore, FIV RNA, the presence of which is an indicator of viral replication, required a highly sensitive nested PCR protocol for detection in FIV-infected brain tissue and was most prevalent in Petaluma-infected animals, suggesting that viral replication in the brain was lower for the more-neurovirulent FIV strains. These findings are consistent with other reports indicating that viral replication in the brain is poorly correlated with the development of neurological disease in FIV-infected adult cats (5, 40) and simian immunodeficiency virus (SIV)-infected neonatal

macaques (58). Furthermore, recent studies have suggested that invasion of the CNS by lentiviruses occurs within days of primary infection and that most neurological damage occurs within the first few weeks (18). Of note, maximal cell death occurred with CM harvested at 3 to 4 days p.i. from infected feline macrophages, further supporting the concept that neuronal injury may be an early phenomenon in FIV infection.

The results presented here support an indirect mechanism for FIV-mediated neuronal injury involving soluble macrophage-derived toxins. Although the results obtained *in vitro* do not necessarily reflect *in vivo* processes, similar patterns were observed in brain tissues from FIV-infected neonates. Although a range of putative neurotoxins have been posited to contribute to lentivirus neuropathogenesis, inhibition of MMP-2 was found to attenuate the neurotoxicity associated with V1CSF and FIVCh infection. Given the roles of MMPs in both physiological and pathological processes, several mechanisms can be envisaged by which these proteins function in FIV neuropathogenesis. Increased BBB permeability, which is associated with the development of FIV-induced neurological disease (39), is promoted by increased CNS expression of either MMP-2 or MMP-9 (46, 60). Alternatively, MMPs produced in the brain may act directly to alter neuronal function, development, and survival, as suggested for other neurological diseases (46, 60). For example, MMP-2 modulates chloride channel activity (16) and hence may influence excitotoxicity caused by neurotransmitters that have been implicated in FIV neuropathogenesis, such as glutamate (4, 6, 20, 61). An indirect mechanism for MMP-induced neuronal damage can also be envisaged, whereby cleavage products of MMP activity mediate the observed neurotoxicity. For example, both MMP-2 and MMP-9 function in the processing of cell surface molecules to yield biologically active precursors with potentially toxic effects, such as the release of soluble TNF- α (17, 57).

This study focused on MMP-2 and -9 as potential mediators of FIV neurotoxicity; however, inhibition of MMP-2 did not prevent this neurotoxicity completely and had little effect on the neuronal death induced by CM from Petaluma-infected MDM. In fact, blocking MMP-2 activity reduced the neurotoxicity exhibited by V1CSF and FIVCh to levels comparable with that of Petaluma, suggesting that other factors produced by macrophages participate in the cascade of cellular events that causes neurodegeneration. For example, other MMPs induced by FIV infection may cause neuronal damage independently, either by acting on their respective substrates or by modulating the activities of other toxic molecules, or may act to augment the toxicity of MMP-2. This potential is illustrated by the fact that the neuronal death caused by HIV type 1 Tat can be inhibited by blocking the function of matrilysin (25), a nonneurotoxic MMP that exhibits the capacity to activate pro-MMP-2 (33, 60). In a similar manner, MMP-2 can activate MMP-1 (33), an enzyme that has been shown to directly kill neurons (56). MMP-9 has not been found to be directly neurotoxic *in vitro* (25, 56), a finding supported by the results of the present study, in which PMT, an inhibitor of both MMP-2 and MMP-9, did not affect the neuronal death caused by Petaluma despite elevated MMP-9 levels following infection of MDM by this virus. However, the failure of MMP-9 to contribute to the *in vitro* neurotoxicity induced by FIV does not preclude a role in the *in vivo* neuropathogenesis of FIV, pos-

sibly by contributing to the BBB breakdown that precedes inflammation and leukocyte infiltration in the CNS. Hence, a cooperative interplay may occur in which several MMPs interact to contribute to FIV-induced neurological disease.

It is important to note that the profiles of FIV infection in FIVCh- and V1CSF-infected neonates were not identical. Despite few significant differences, FIVCh was also less neurovirulent. V1CSF infection of MDM resulted in increased neurotoxicity *in vitro*, and microglial nodules were more apparent in V1CSF-infected neonatal brain tissue. In addition, V1CSF-infected cats had higher MDS scores and differed from FIVCh animals in the degree to which performance of tasks was impaired, in some instances completely lacking the ability to perform the task (data not shown). Since FIVCh shares only the envelope gene of V1CSF, these results may indicate differences in other viral genes, such as *vif* or *ORFA*, a putative *tat* homologue. Both of these genes, which are conserved between FIVCh and Petaluma, have been shown to influence FIV replication in primary cells and *in vivo* pathogenesis (22). Furthermore, the neurotoxicity associated with HIV Tat, which also influences the expression of MMP-2 and -9, can be attenuated by inhibition of MMP-2 activity (25). Thus, as has been proposed for HIV (34), FIV-induced neurological diseases may be the product of the cumulative or synergistic effect of several viral proteins.

Despite neuronal death *in vitro*, limited neuronal loss was apparent *in vivo*, raising questions as to the relevance of *in vitro* neurotoxicity to the neuropathogenesis of FIV strains. These findings may reflect the absence *in vitro* of other neural cells or factors with neuroprotective properties, such as the production of neurotrophins by astrocytes (7). Alternatively, neurons within the developing nervous system may be susceptible to the functional impairment induced by FIV infection but more resistant to structural injury leading to death than the terminally differentiated neuronal cell line used in this study. For example, infection of adult cats by V1CSF and Petaluma has been shown previously to lead to neuronal loss (44). In support of this concept, neuronal damage that manifested as dysmorphic cell bodies and truncated cellular processes was more prominent in brain tissues from V1CSF- and FIVCh-infected animals than in those from Petaluma-infected cats. In addition, expression of the transcription factor *c-fos* was increased in brain tissues from animals infected with neurovirulent FIV strains. Previously, *c-fos* expression has been shown to be upregulated in response to brain injury and excitotoxic insult, potentially contributing to the initiation of apoptosis in neurons (19, 35). It is interesting that *c-fos* also regulates MMP expression (13, 50) and activates the FIV long terminal repeat (32).

The results of these studies demonstrate that specific sequences in the FIV envelope gene have the capacity to confer a virulent phenotype *in vivo*, influencing the development of both immunological and neurological impairment. Together with a role for MMP-2 in the neurotoxicity exhibited by FIV, these results suggest that envelope-mediated upregulation of MMP expression is a property common to the neuropathogenesis of FIV and HIV, supporting the concept that evolutionarily distinct lentiviruses retain conserved mechanisms of infection and virulence. By nature, studies of HIV-associated neurological disease must focus on events occurring near the

terminal stages of infection, a restriction due in part to the difficulties inherent to identifying and characterizing patients immediately following initial exposure to the virus. A recent report using the SIV-macaque model has suggested that the early events of CNS entry and neuronal damage are essential to the development of neurological disease (18). Hence, the virus-host relationships established in the early stages of infection are critical determinants of disease outcome and progression. Therefore, the FIV system may provide a potential animal model for targeting molecules for future neuroprotective treatments in diseases involving MMPs, such as HIV-AIDS.

ACKNOWLEDGMENTS

We thank Colleen Geary and Aundria Ford for animal care assistance and David Shalinsky (Agouron) for providing PMT.

These studies were supported by the Canadian Institute for Health Research (CIHR), the Natural Sciences and Engineering Research Council of Canada (NSERC), and the Alberta Heritage Foundation for Medical Research (AHFMR).

REFERENCES

- Bachmann, M. H., C. Mathiason-Dubard, G. H. Learn, A. G. Rodrigo, D. L. Sodora, P. Mazzetti, E. A. Hoover, and J. I. Mullins. 1997. Genetic diversity of feline immunodeficiency virus: dual infection, recombination, and distinct evolutionary rates among envelope sequence clades. *J. Virol.* **71**:4241–4253.
- Bendinelli, M., M. Pistello, S. Lombardi, A. Poli, C. Garzelli, D. Matteucci, L. Ceccherini-Nelli, G. Malvaldi, and F. Tozzini. 1995. Feline immunodeficiency virus: an interesting model for AIDS studies and an important cat pathogen. *Clin. Microbiol. Rev.* **8**:87–112.
- Berman, N. E., J. K. Marcario, C. Yong, R. Raghavan, L. A. Raymond, S. V. Joag, O. Narayan, and P. D. Cheney. 1999. Microglial activation and neurological symptoms in the SIV model of NeuroAIDS: association of MHC-II and MMP-9 expression with behavioral deficits and evoked potential changes. *Neurobiol. Dis.* **6**:486–498.
- Billaud, J. N., D. Selway, N. Yu, and T. R. Phillips. 2000. Replication rate of feline immunodeficiency virus in astrocytes is envelope dependent: implications for glutamate uptake. *Virology* **266**:180–188.
- Boche, D., M. Hurtrel, F. Gray, M. A. Claessens Maire, J. P. Ganiere, L. Montagnier, and B. Hurtrel. 1996. Virus load and neuropathology in the FIV model. *J. Neurovirol.* **2**:377–387.
- Bragg, D. C., R. B. Meeker, B. A. Duff, R. V. English, and M. B. Tompkins. 1999. Neurotoxicity of FIV and FIV envelope protein in feline cortical cultures. *Brain Res.* **816**:431–437.
- Breneman, D. E., T. M. Phillips, B. W. Festoff, and I. Gozes. 1997. Identity of neurotrophic molecules released from astroglia by vasoactive intestinal peptide. *Ann. N. Y. Acad. Sci.* **814**:167–173.
- Burns, D. P., and R. C. Desrosiers. 1991. Selection of genetic variants of simian immunodeficiency virus in persistently infected rhesus monkeys. *J. Virol.* **65**:1843–1854.
- Chesebro, B., K. Wehrly, J. Nishio, and S. Perryman. 1992. Macrophage-tropic human immunodeficiency virus isolates from different patients exhibit unusual V3 envelope sequence homogeneity in comparison with T-cell-tropic isolates: definition of critical amino acids involved in cell tropism. *J. Virol.* **66**:6547–6554.
- Cichutek, K., H. Merget, S. Norley, R. Linde, W. Kreuz, M. Gahr, and R. Kurth. 1992. Development of a quasispecies of human immunodeficiency virus type 1 *in vivo*. *Proc. Natl. Acad. Sci. USA* **89**:7365–7369.
- Clements, J. E., F. S. Pedersen, O. Narayan, and W. A. Haseltine. 1980. Genomic changes associated with antigenic variation of visna virus during persistent infection. *Proc. Natl. Acad. Sci. USA* **77**:4454–4458.
- Conant, K., J. C. McArthur, D. E. Griffin, L. Sjulson, L. M. Wahl, and D. N. Irani. 1999. Cerebrospinal fluid levels of MMP-2, -7, and -9 are elevated in association with human immunodeficiency virus dementia. *Ann. Neurol.* **46**:391–398.
- Crowe, D. L., and T. N. Brown. 1999. Transcriptional inhibition of matrix metalloproteinase 9 (MMP-9) activity by a *c-fos*/estrogen receptor fusion protein is mediated by the proximal AP-1 site of the MMP-9 promoter and correlates with reduced tumor cell invasion. *Neoplasia* **1**:368–372.
- Cunningham, A. L., H. Naif, N. Saksena, G. Lynch, J. Chang, S. Li, R. Jozwiak, M. Alali, B. Wang, W. Fear, A. Sloane, L. Pemberton, and B. Brew. 1997. HIV infection of macrophages and pathogenesis of AIDS dementia complex: interaction of the host cell and viral genotype. *J. Leukoc. Biol.* **62**:117–125.
- Dow, S. W., M. L. Poss, and E. A. Hoover. 1990. Feline immunodeficiency virus: a neurotropic lentivirus. *J. Acquir. Immune Defic. Syndr.* **3**:658–668.

16. Duszyk, M., Y. Shu, G. Sawicki, A. Radomski, S. F. Man, and M. W. Radomski. 1999. Inhibition of matrix metalloproteinase MMP-2 activates chloride current in human airway epithelial cells. *Can. J. Physiol. Pharmacol.* **77**:529–535.
17. Gearing, A. J., P. Beckett, M. Christodoulou, M. Churchill, J. M. Clements, M. Crimmin, A. H. Davidson, A. H. Drummond, W. A. Galloway, R. Gilbert, et al. 1995. Matrix metalloproteinases and processing of pro-TNF- α . *J. Leukoc. Biol.* **57**:774–777.
18. Gonzalez, R. G., L. L. Cheng, S. V. Westmoreland, K. E. Sakaie, L. R. Becerra, P. L. Lee, E. Masliah, and A. A. Lackner. 2000. Early brain injury in the SIV-macaque model of AIDS. *AIDS* **14**:2841–2849.
19. Griffiths, R., C. Malcolm, L. Ritchie, A. Frandsen, A. Schousboe, M. Scott, P. Rumsby, and C. Meredith. 1997. Association of *c-fos* mRNA expression and excitotoxicity in primary cultures of mouse neocortical and cerebellar neurons. *J. Neurosci. Res.* **48**:533–542.
20. Grulic, D. L., N. Yu, K. L. Parsons, J. N. Billaud, J. H. Elder, and T. R. Phillips. 1998. Neurotoxic effects of feline immunodeficiency virus, FIV-PPR. *J. Neurovirol.* **4**:415–425.
21. Heseltine, P. N., K. Goodkin, J. H. Atkinson, B. Vitiello, J. Rochon, R. K. Heaton, E. M. Eaton, F. L. Wilkie, E. Sobel, S. J. Brown, D. Feaster, L. Schneider, W. L. Goldschmidt, and E. S. Stover. 1998. Randomized double-blind placebo-controlled trial of peptide T for HIV-associated cognitive impairment. *Arch. Neurol.* **55**:41–51.
22. Inoshima, Y., M. Kohmoto, Y. Ikeda, H. Yamada, Y. Kawaguchi, K. Tomonaga, T. Miyazawa, C. Kai, T. Umemura, and T. Mikami. 1996. Roles of the auxiliary genes and AP-1 binding site in the long terminal repeat of feline immunodeficiency virus in the early stage of infection in cats. *J. Virol.* **70**:8518–8526.
23. Johnston, J., and C. Power. 1999. Productive infection of human peripheral blood mononuclear cells by feline immunodeficiency virus: implications for vector development. *J. Virol.* **73**:2491–2498.
24. Johnston, J. B., Y. Jiang, G. van Marle, M. B. Mayne, W. Ni, J. Holden, J. C. McArthur, and C. Power. 2000. Lentivirus infection in the brain induces matrix metalloproteinase expression: role of envelope diversity. *J. Virol.* **74**:7211–7220.
25. Johnston, J. B., K. Zhang, C. Silva, D. R. Shalinsky, K. Conant, W. Ni, D. Corbett, V. W. Yong, and C. Power. 2001. HIV-1 Tat neurotoxicity is prevented by matrix metalloproteinase inhibitors. *Ann. Neurol.* **49**:230–241.
26. Khanna, K. V., X. F. Yu, D. H. Ford, L. Ratner, J. K. Hildreth, and R. B. Markham. 2000. Differences among HIV-1 variants in their ability to elicit secretion of TNF- α . *J. Immunol.* **164**:1408–1415.
27. Kim, C. H., and J. W. Casey. 1992. Genomic variation and segregation of equine infectious anemia virus during acute infection. *J. Virol.* **66**:3879–3882.
28. Kolkenbrock, H., A. Hecker-Kia, D. Orgel, N. Ulbrich, and N. Will. 1997. Activation of progelatinase A and progelatinase A/TIMP-2 complex by membrane type 2-matrix metalloproteinase. *Biol. Chem.* **378**:71–76.
29. Kong, L. Y., B. C. Wilson, M. K. McMillian, G. Bing, P. M. Hudson, and J. S. Hong. 1996. The effects of the HIV-1 envelope protein gp120 on the production of nitric oxide and proinflammatory cytokines in mixed glial cell cultures. *Cell. Immunol.* **172**:77–83.
30. Lerner, D. L., and J. H. Elder. 2000. Expanded host cell tropism and cytopathic properties of feline immunodeficiency virus strain PPR subsequent to passage through interleukin-2-independent T cells. *J. Virol.* **74**:1854–1863.
31. Mankowski, J. L., M. T. Flaherty, J. P. Spelman, D. A. Hauer, P. J. Didier, A. M. Amedee, M. Murphey-Corb, L. M. Kirstein, A. Munoz, J. E. Clements, and M. C. Zink. 1997. Pathogenesis of simian immunodeficiency virus encephalitis: viral determinants of neurovirulence. *J. Virol.* **71**:6055–6060.
32. Miyazawa, T., M. Kohmoto, Y. Kawaguchi, K. Tomonaga, T. Toyosaki, K. Ikuta, A. Adachi, and T. Mikami. 1993. The AP-1 binding site in the feline immunodeficiency virus long terminal repeat is not required for virus replication in feline T lymphocytes. *J. Gen. Virol.* **74**:1573–1580.
33. Nagase, H. 1997. Activation mechanisms of matrix metalloproteinases. *Biol. Chem.* **378**:151–160.
34. Nath, A., N. J. Haughey, M. Jones, C. Anderson, J. E. Bell, and J. D. Geiger. 2000. Synergistic neurotoxicity by human immunodeficiency virus proteins Tat and gp120: protection by memantine. *Ann. Neurol.* **47**:186–194.
35. Oo, T. F., C. Henchcliffe, D. James, and R. E. Burke. 1999. Expression of *c-fos*, *c-jun*, and *c-jun* N-terminal kinase (JNK) in a developmental model of induced apoptotic death in neurons of the substantia nigra. *J. Neurochem.* **72**:557–564.
36. Pancino, G., S. Castlot, and P. Sonigo. 1995. Differences in feline immunodeficiency virus host cell range correlate with envelope fusogenic properties. *Virology* **206**:796–806.
37. Pedersen, N. C., E. W. Ho, M. L. Brown, and J. K. Yamamoto. 1987. Isolation of a T-lymphotropic virus from domestic cats with an immunodeficiency-like syndrome. *Science* **235**:790–793.
38. Phillips, T. R., O. Prospero-Garcia, D. L. Puaoi, D. L. Lerner, H. S. Fox, R. A. Olmsted, F. E. Bloom, S. J. Henriksen, and J. H. Elder. 1994. Neurological abnormalities associated with feline immunodeficiency virus infection. *J. Gen. Virol.* **75**:979–987.
39. Podell, M., K. Hayes, M. Oglesbee, and L. Mathes. 1997. Progressive encephalopathy associated with CD4/CD8 inversion in adult FIV-infected cats. *J. Acquir. Immune Defic. Syndr. Hum. Retrovirol.* **15**:332–340.
40. Poli, A., M. Pistello, M. A. Carli, F. Abramo, G. Mancuso, E. Nicoletti, and M. Bendinelli. 1999. Tumor necrosis factor- α and virus expression in the central nervous system of cats infected with feline immunodeficiency virus. *J. Neurovirol.* **5**:465–473.
41. Power, C., R. Buist, J. B. Johnston, M. R. Del Bigio, W. Ni, M. R. Dawood, and J. Peeling. 1998. Neurovirulence in feline immunodeficiency virus-infected neonatal cats is viral strain specific and dependent on systemic immune suppression. *J. Virol.* **72**:9109–9115.
42. Power, C., J. C. McArthur, R. T. Johnson, D. E. Griffin, J. D. Glass, R. Dewey, and B. Chesebro. 1995. Distinct HIV-1 env sequences are associated with neurotropism and neurovirulence. *Curr. Top. Microbiol. Immunol.* **202**:89–104.
43. Power, C., J. C. McArthur, A. Nath, K. Wehrly, M. Mayne, J. Nishio, T. Langelier, R. T. Johnson, and B. Chesebro. 1998. Neuronal death induced by brain-derived human immunodeficiency virus type 1 envelope genes differs between demented and nondemented AIDS patients. *J. Virol.* **72**:9045–9053.
44. Power, C., T. Moench, J. Peeling, P. A. Kong, and T. Langelier. 1997. Feline immunodeficiency virus causes increased glutamate levels and neuronal loss in brain. *Neuroscience* **77**:1175–1185.
45. Prospero-Garcia, O., S. Huitron-Resendiz, S. C. Caselman, M. Sanchez-Alavez, O. Diaz-Ruiz, L. Navarro, D. L. Lerner, T. R. Phillips, J. H. Elder, and S. J. Henriksen. 1999. Feline immunodeficiency virus envelope protein (FIV gp120) causes electrophysiological alterations in rats. *Brain Res.* **836**:203–209.
46. Rosenberg, G. A. 1995. Matrix metalloproteinases in brain injury. *J. Neurotrauma* **12**:833–842.
47. Shalinsky, D. R., J. Brekken, H. Zou, C. D. McDermott, P. Forsyth, D. Edwards, S. Margosiak, S. Bender, G. Truitt, A. Wood, N. M. Varki, and K. Appelt. 1999. Broad antitumor and antiangiogenic activities of AG3340, a potent and selective MMP inhibitor undergoing advanced oncology clinical trials. *Ann. N. Y. Acad. Sci.* **878**:236–270.
48. Strizki, J. M., A. V. Albright, H. Sheng, M. O'Connor, L. Perrin, and F. Gonzalez-Scarano. 1996. Infection of primary human microglia and monocyte-derived macrophages with human immunodeficiency virus type 1 isolates: evidence of differential tropism. *J. Virol.* **70**:7654–7662.
49. Torsteinsdottir, S., G. Agnarsdottir, S. Matthiasdottir, B. Rafnar, V. Andressdottir, O. S. Andresson, K. Staskus, G. Petursson, P. A. Palsson, and G. Georgsson. 1997. In vivo and in vitro infection with two different molecular clones of visna virus. *Virology* **229**:370–380.
50. Tsuji, M., K. Hirakawa, A. Kato, and K. Fujii. 2000. The possible role of *c-fos* expression in rheumatoid cartilage destruction. *J. Rheumatol.* **27**:1606–1621.
51. Uhm, J. H., N. P. Dooley, J. G. Villemure, and V. W. Yong. 1996. Glioma invasion in vitro: regulation by matrix metalloproteinase-2 and protein kinase C. *Clin. Exp. Metastasis* **14**:421–433.
52. Vahlenkamp, T. W., A. de Ronde, N. N. Schuurman, A. L. van Vliet, J. van Druenen, M. C. Horzinek, and H. F. Egberink. 1999. Envelope gene sequences encoding variable regions 3 and 4 are involved in macrophage tropism of feline immunodeficiency virus. *J. Gen. Virol.* **80**:2639–2646.
53. Vahlenkamp, T. W., E. J. Verschoor, N. N. Schuurman, A. L. van Vliet, M. C. Horzinek, H. F. Egberink, and A. de Ronde. 1997. A single amino acid substitution in the transmembrane envelope glycoprotein of feline immunodeficiency virus alters cellular tropism. *J. Virol.* **71**:7132–7135.
54. Verschoor, E. J., L. A. Boven, H. Blaak, A. L. van Vliet, M. C. Horzinek, and A. de Ronde. 1995. A single mutation within the V3 envelope neutralization domain of feline immunodeficiency virus determines its tropism for CRFK cells. *J. Virol.* **69**:4752–4757.
55. Vitkovic, L., E. Stover, and S. H. Koslow. 1995. Animal models recapitulate aspects of HIV/CNS disease. *AIDS Res. Hum. Retrovir.* **11**:753–759.
56. Vos, C. M., L. Sjulson, A. Nath, J. C. McArthur, C. A. Pardo, J. Rothstein, and K. Conant. 2000. Cytotoxicity by matrix metalloproteinase-1 in organotypic spinal cord and dissociated neuronal cultures. *Exp. Neurol.* **163**:324–330.
57. Watanabe, N., K. Nakada, and Y. Kobayashi. 1998. Processing and release of tumor necrosis factor alpha. *Eur. J. Biochem.* **253**:576–582.
58. Westmoreland, S. V., K. C. Williams, M. A. Simon, M. E. Bahn, A. E. Rullkoetter, M. W. Elliott, C. D. deBakker, H. L. Knight, and A. A. Lackner. 1999. Neuropathogenesis of simian immunodeficiency virus in neonatal rhesus macaques. *Am. J. Pathol.* **155**:1217–1228.
59. Willett, B. J., and M. J. Hosie. 1999. The role of the chemokine receptor CXCR4 in infection with feline immunodeficiency virus. *Mol. Membr. Biol.* **16**:67–72.
60. Yong, V. W., C. A. Krekoski, P. A. Forsyth, R. Bell, and D. R. Edwards. 1998. Matrix metalloproteinases and diseases of the CNS. *Trends Neurosci.* **21**:75–80.
61. Yu, N., J. N. Billaud, and T. R. Phillips. 1998. Effects of feline immunodeficiency virus on astrocyte glutamate uptake: implications for lentivirus-induced central nervous system diseases. *Proc. Natl. Acad. Sci. USA* **95**:2624–2629.
62. Zenger, E., E. Tiffany-Castiglioni, and E. W. Collisson. 1997. Cellular mechanisms of feline immunodeficiency virus (FIV)-induced neuropathogenesis. *Front. Biosci.* **2**:d527–d537.